3532 BULLETIN OF THE CHEMICAL SOCIETY OF JAPAN, VOL. 52 (12), 3532—3538 (1979) [Vol. 52, No. 12]

Kinetics and Mechanism of the Oxidation Reactions of Dialkyldithiocarbamatocopper(I) Tetramer and -silver(I) Hexamer with Tetraalkylthiuram Disulfide

Hidetoshi KITA, Shin-ichi MIYAKE, Koji TANAKA, and Toshio TANAKA*

Department of Applied Chemistry, Faculty of Engineering, Osaka University, Suita, Osaka 565

(Received February 19 1979)

Kinetics of the oxidations of dialkyldithiocarbamatocopper(I), $[\{Cu(S_2CNR_2)\}_4]$ (R=Et, *n*-Pr), and -silver(I), $[\{Ag(S_2CNR_2)\}_6]$ (R=Et, *n*-Pr, *i*-Pr), with the corresponding tetraalkylthiuram disulfide, $[(R_2NC(S)S\}_2]$, were investigated in dichloromethane employing a stopped-flow technique. The reactions are interpreted to proceed by a mechanism involving a rapid equilibration (**i**) (the multi-step equilibrium constant=K_0) to form adduct,

$$[\{M(S_2CNR_2)\}_x] \xrightleftharpoons{+[(R_2NC(S)S\}_2]} [M(S_2CNR_2)\{(R_2NC(S)S\}_2\}] + [\{M(S_2CNR_2)\}_{x-1}] \xrightleftharpoons{+[(R_2NC(S)S\}_2]} \cdots \quad (\mathbf{i})$$

(M=Cu, x=4; M=Ag, x=6)

$[M(S_2CNR_2)\{(R_2NC(S)S\}_2\}]$, which are decomposed in a rate-determining step (the rate constant=k) yielding the final products, $[M(S_2CNR_2)_2]$. According to this mechanism, the rate law in the presence of excess $[(R_2NC(S)S\}_2]$ is expressed as $v=K_0k[[(R_2NC(S)S\}_2]][[\{M(S_2CNR_2)\}_x]]/(1+K_0[[(R_2NC(S)S\}_2]])$, where K_0k(25 °C)$=1.17\times10^4$ (Et), 5.70×10^3 (*n*-Pr) $M^{-1}\,s^{-1}$ (M=mol dm^{-3}) for the copper system, and K_0(25 °C)=28.2 (Et), 49.1 (*n*-Pr), 86.7 (*i*-Pr) M^{-1} and k(25 °C)=2.17 (Et), 1.50 (*n*-Pr), 6.56 (*i*-Pr) s^{-1} for the silver system. The activation parameters also were determined and the nature of transition states is discussed.

The dithiocarbamate ligand can stabilize transition metal ions in unusually high formal oxidation states by delocalization of electronic charges[1)] and S–S interligand interactions,[2)] as shown in the canonical structures of **b** and **c**, respectively.

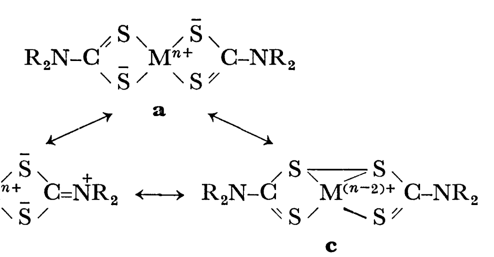

This interesting property seems to facilitate a number of studies[3–9)] on the reaction of dithiocarbamato complexes of metals in the normal oxidation state with oxidizing agents such as halogens, boron trifluoride *etc*. All the works reported in this field, however, had been of a preparative nature until recently. Thus, we have reported the kinetics and mechanism of the oxidation reactions of dithiocarbamato complexes of tin(IV),[10)] zinc(II),[11)] and gold(I)[12)] with halogens. These reactions have well been described to proceed *via* a charge-transfer complex formed by electrophilic attack of halogen on the sulfur atom of the dithiocarbamate ligand. As an extension of these studies to more complicated systems, the present paper reports kinetic and mechanistic studies on the oxidation reactions of dialkyldithiocarbamatocopper(I) tetramer and -silver(I) hexamer with tetraalkylthiuram disulfide, giving bis(dialkyldithiocarbamato)copper(II) and -silver(II), respectively.

Experimental

Materials. Dialkyldithiocarbamatocopper(I), $[\{Cu(S_2CNR_2)\}_4]$ (R=Et and *n*-Pr),[13)] dialkyldithiocarbamatosilver(I), $[\{Ag(S_2CNR_2)\}_6]$ (R=Et, *n*-Pr, and *i*-Pr),[14)] and tetraalkylthiuram disulfide, $[(R_2NC(S)S\}_2]$ (R=Et, *n*-Pr, and *i*-Pr),[14)] were prepared according to the literature methods. Analytical data for these complexes (C, H, N) were satisfactory. Dichloromethane used as a solvent was purified as described previously.[12)]

Spectra and Kinetics. Electronic spectra were recorded on a Hitachi 124 spectrophotometer. Rapid scanning spectra were measured with a Union RA-413 stopped-flow rapid scanning spectrophotometer equipped with a 2 mm quartz cell in a cell holder thermostated within ±0.2 °C. The rate of reaction was followed by monitoring the absorbance at a fixed wavelength in the electronic spectra of the reaction mixture under pseudo-first-order conditions, using at least a ten-fold excess of tetraalkylthiuram disulfide. Absorbance-time data were accumulated at least five times on a Union System-71 data processor and average absorbance-time curves were recorded on a National VP-6421A X-Y recorder. Pseudo-first-order rate constants, k_{obsd}, were calculated from the slope of a linear part of the $\ln(A_\infty - A_t)$ *vs.* time plots by the least-squares method, where A_∞ and A_t are absorbances at the end of reaction and at a time t, respectively.

Results and Discussion

Reaction of $[\{Cu(S_2CNR_2)\}_4]$ *with* $[(R_2NC(S)S\}_2]$. The reaction of $[\{Cu(S_2CNR_2)\}_4]$ with $[(R_2NC(S)S\}_2]$ rapidly proceeds to give bis(dialkyldithiocarbamato)copper(II), $[Cu(S_2CNR_2)_2]$, in quantitative yields.[15)] The stoichiometry of reaction can, therefore, be expressed as Eq. 1.

$$\frac{1}{4}[\{Cu(S_2CNR_2)\}_4] + \frac{1}{2}[(R_2NC(S)S\}_2] \longrightarrow [Cu(S_2CNR_2)_2] \quad (1)$$

A typical rapid scanning spectrum after mixing the reactant solutions is shown in Fig. 1. An absorption maximum at 303 nm observed immediately after mixing is identical in wavenumber with that of the

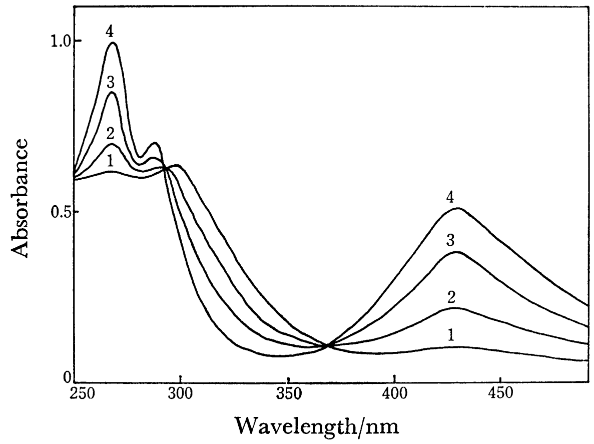

Fig. 1. Rapid scanning spectra after mixing $[\{Cu(S_2CNEt_2)\}_4]$ (5.1×10^{-5} M) with $[(Et_2NC(S)S\}_2]$ (1.0×10^{-4} M) in CH_2Cl_2 at 25 °C; cell length=2 mm. 1: 0.5 s, 2: 1.0 s, 3: 2.0 s, 4: the end of reaction.

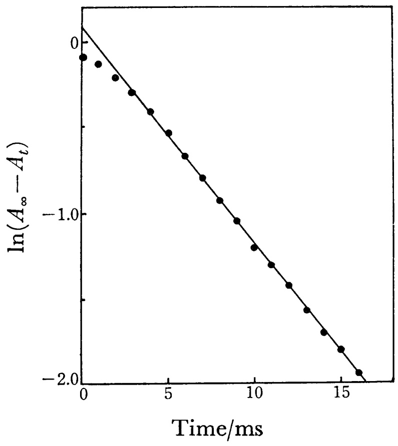

Fig. 2. Plots of $\ln(A_\infty - A_t)$ *vs.* time at 25 °C: $[[\{Cu(S_2CNEt_2)\}_4]] = 1.0\times10^{-4}$ M, $[[(Et_2NC(S)S\}_2]] = 1.0\times10^{-2}$ M; cell length=2 mm.

Table 1. Pseudo-first-order rate constants for the reaction of $[\{Cu(S_2CNR_2)\}_4]$ with $[(R_2NC(S)S\}_2]$ in CH_2Cl_2

R	Temp/°C	$10^4[[\{Cu(S_2CNR_2)\}_4]]$/M	$10^4[[(R_2NC(S)S\}_2]]$/M	k_{obsd}/s^{-1}
Et	10.5	0.501	20.0	12.8
			40.0	28.0
			59.7	44.3
			80.9	59.3
			100	73.5
	12.5	1.00	100	82.8
			200	156
			301	264
			400	314
			500	413
	15.5	0.501	20.0	18.4
			40.0	33.6
			59.7	48.8
			80.9	70.4
			100	89.0
	16.9	1.00	100	100
			200	214
			301	317
			400	450
			500	523
	20.1	0.501	20.0	24.9
			40.0	43.9
			59.7	65.4
			80.9	83.1
		1.00	100	115
			200	243
			301	312
			400	481
	25.0	0.505	10.0	14.3
		1.51	20.1	18.8
		0.625	25.0	38.2
		0.505	40.0	52.3
			50.1	66.3
			80.0	93.4
		1.00	100	127
			200	245
			301	349
n-Pr	10.9	0.529	20.8	6.37
			40.0	13.6
			60.4	21.3
			79.7	28.2
			99.8	35.3
	15.8	0.529	20.8	7.31
			40.0	17.3
			60.4	23.7
			79.7	32.1
			99.8	42.3
	20.3	0.513	20.1	11.5
			40.0	23.0
			50.1	29.1
			61.5	36.8
		0.529	60.4	31.6
			79.7	39.7
			100	50.4
		1.08	100	51.9
			203	94.4
			302	151
			401	195
			500	221
	25.0	1.28	20.1	14.7
		0.513	39.8	25.5
		1.28		28.7
		0.513	50.1	33.1
		1.28		37.0
		0.513	61.5	44.3
		1.28		42.3
		0.513	79.7	53.7
			100	65.5
		1.08	100	63.4
		0.513	123	74.7
		1.08	203	134
			302	192
			401	244
			500	276

reactant $[\{Cu(S_2CNR_2)\}_4]$ ($\lambda_{max}=303$ nm, $\varepsilon_{max}=4.5\times10^4\ M^{-1}\,cm^{-1}$ ($M=mol\ dm^{-3}$) in CH_2Cl_2). The final spectrum with three absorption peaks at 270, 290, and 435 nm is assigned to $[Cu(S_2CNR_2)_2]$ ($\varepsilon_{max}=3.1\times10^4$, 1.8×10^4, and $1.2\times10^4\ M^{-1}\,cm^{-1}$ in CH_2Cl_2, respectively).[15-18] Half-lives of these absorption bands were almost identical with one another, and isosbestic points are found at 295 and 370 nm.

The rate data of reaction 1 (R=Et and *n*-Pr) were obtained from increase of the absorbance at 435 nm after mixing $[\{Cu(S_2CNR_2)\}_4]$ with excess $[(R_2NC(S)S\}_2]$. Figure 2 shows a typical example of $\ln(A_\infty-A_t)$ *vs.* time plots. Except for the period of initial several milliseconds, a good linear relation between them is obtained for at least 80% completion of the reaction. The linear part of plots was used to determine the values of pseudo-first-order rate constants. Table 1 lists the rate data at various concentrations of $[\{Cu(S_2CNR_2)\}_4]$ and $[(R_2NC(S)S\}_2]$. All the plots of k_{obsd} *vs.* the concentration of $[(R_2NC(S)\}_2]$ at each temperature yielded straight lines with zero intercepts. This result may be interpreted by assuming the reaction pathways of 2 to 4.

$$[\{Cu(S_2CNR_2)\}_4] \xrightleftharpoons{+[(R_2NC(S)S\}_2]} [Cu(S_2CNR_2)\{(R_2NC(S)S\}_2\}] + [\{Cu(S_2CNR_2)\}_3] \xrightleftharpoons{+[(R_2NC(S)S\}_2]} \cdots\cdots \quad K_0, \qquad (2)$$

$$[Cu(S_2CNR_2)\{(R_2NC(S)S\}_2\}] \xrightarrow{k} [Cu(S_2CNR_2)_2] + [R_2NCS_2\cdot] \qquad (3)$$

$$2[R_2NCS_2\cdot] \xrightarrow{fast} [(R_2NC(S)S\}_2] \qquad (4)$$

Equation 2 consists of multi-step equilibrium reactions, where the tetrameric compound $[\{Cu(S_2CNR_2)\}_4]$ dissociates by the attack of $[(R_2NC(S)S\}_2]$ to form an adduct $[Cu(S_2CNR_2)\{(R_2NC(S)S\}_2\}]$ and a trimer $[\{Cu(S_2CNR_2)\}_3]$, the latter of which successively reacts with $[(R_2NC(S)S\}_2]$ to give the adduct in a similar manner. The initial curvature of $\ln(A_\infty-A_t)$ *vs.* time plots (Fig. 2) may correspond to a preequilibrium immediately after mixing, where the concentration of the adduct does not reach a steady state. The formation of the adduct as an intermediate may be supported by the fact that several metal complexes of thiuram disulfide have been isolated,[19-21] although there is no direct evidence in the present study. Thus, two possible structures, **1** and **2**, are proposed for the adduct formed between the copper(I) complex and thiuram disulfide.

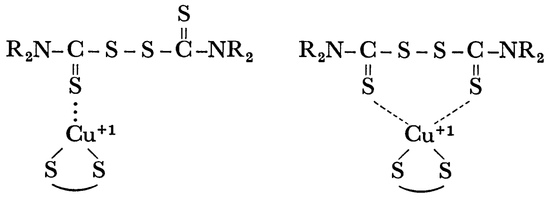

1: $\overset{\frown}{S\quad S}=S_2CNR_2$ **2**

In either structure the adduct may be decomposed in a rate-determining step (Eq. 3), which involves homolytic cleavage of the S–S bond of tetraalkylthiuram disulfide to give the oxidized copper(II) product, $[Cu(S_2CNR_2)_2]$, and the $[R_2NCS_2\cdot]$ radical. The resulting radical may rapidly dimerize to regenerate tetraalkylthiuram disulfide as reported by Cauquis and Lachenal,[22] who have estimated the rate constant of dimerization for R=Et to be $2\times10^5\ M^{-1}\,s^{-1}$ in acetonitrile.

According to the pathways of 2—4, the k_{obsd} value in the presence of excess tetraalkylthiuram disulfide is expressed by Eq. 5,

$$k_{obsd}=\frac{K_0k[[(R_2NC(S)S\}_2]]}{1+K_0[[(R_2NC(S)S\}_2]]}, \qquad (5)$$

where K_0 stands for the multi-step equilibrium constant in Eq. 2. If one assumes $K_0[[(R_2NC(S)S\}_2]]\ll1$, Eq. 5 can be reduced to Eq. 6,

$$k_{obsd}=K_0k[[(R_2NC(S)S\}_2]] \qquad (6)$$

which predicts a linear relationship between k_{obsd} and the concentration of $[(R_2NC(S)S\}_2]$ with the slope of K_0k and the zero intercept. This is consistent with the observed rate profile. Table 2 lists the K_0k value and activation parameters determined from the Arrhenius plot of $\ln(K_0k)$ *vs.* $1/T$.

Reaction of $[\{Ag(S_2CNR_2)\}_6]$ *with* $[(R_2NC(S)S\}_2]$. The addition of a dichloromethane solution of $[(R_2NC(S)\}_2]$ to $[\{Ag(S_2CNR_2)\}_6]$ in dichloromethane immediately causes a blue color, which becomes more intense as more $[(R_2NC(S)S\}_2]$ is added. The electronic spectrum of the blue solution displayed an

TABLE 2. KINETIC AND ACTIVATION PARAMETERS FOR THE REACTION OF $[\{Cu(S_2CNR_2)\}_4]$ WITH $[(R_2NC(S)S\}_2]$ IN CH_2Cl_2[a)]

R	Temp °C	K_0k $M^{-1}\,s^{-1}$	$\Delta H^{\neq}$ $kJ\ mol^{-1}$	$\Delta S^{\neq}$ $J\ mol^{-1}K^{-1}$
Et	25.0	$(1.17\pm0.02)\times10^4$	20.6±4.4	−97±10
	20.1	$(1.17\pm0.05)\times10^4$		
	16.9	$(1.08\pm0.05)\times10^4$		
	15.5	$(8.86\pm0.35)\times10^3$		
	12.5	$(8.19\pm0.44)\times10^3$		
	10.5	$(7.60\pm0.11)\times10^3$		
n-Pr	25.0	$(5.70\pm0.09)\times10^3$	18.2±3.1	−112±10
	20.3	$(4.52\pm0.10)\times10^3$		
	15.8	$(4.29\pm0.19)\times10^3$		
	10.9	$(3.67\pm0.03)\times10^3$		

a) Errors quoted are standard deviations.

TABLE 3. EQUILIBRIUM CONSTANTS AND THERMODYNAMIC PARAMETERS FOR THE REACTION OF $[\{Ag(S_2CNR_2)\}_6]$ WITH $[(R_2NC(S)S)_2]$ IN CH_2Cl_2[a)]

R	Temp / °C	K / $M^{1/3}$	ΔH° / kJ mol^{-1}	ΔS° / J mol^{-1}K^{-1}
Et	25.8	$(4.46\pm0.23)\times10^{-4}$	23.0 ± 1.0	12.9 ± 7.4
	20.5	$(3.80\pm0.22)\times10^{-4}$ (3.8×10^{-4})[b)]		
	15.1	$(3.14\pm0.24)\times10^{-4}$		
	10.0	$(2.71\pm0.27)\times10^{-4}$		
n-Pr	24.7	$(4.85\pm0.32)\times10^{-4}$	27.9 ± 0.4	30.2 ± 3.1
	20.4	$(4.16\pm0.34)\times10^{-4}$ (5.5×10^{-4})[b)]		
	15.5	$(3.51\pm0.29)\times10^{-4}$		
	9.7	$(2.66\pm0.34)\times10^{-4}$		
i-Pr	24.6	$(9.21\pm0.13)\times10^{-3}$	16.4 ± 0.4	16.2 ± 3.3
	20.6	$(8.43\pm0.34)\times10^{-3}$ (1.1×10^{-2})[b)]		
	15.3	$(7.35\pm0.35)\times10^{-3}$		
	11.0	$(6.65\pm0.26)\times10^{-3}$		

a) Errors quoted are standard deviations.
b) In $CHCl_3$ at 20 °C; Ref. 15.

TABLE 4. PSEUDO-FIRST-ORDER RATE CONSTANTS FOR THE REACTION OF $[\{Ag(S_2CNR_2)\}_6]$ WITH $[(R_2NC(S)S)_2]$ IN CH_2Cl_2

R	Temp / °C	10^4 $[[Ag\{(S_2CNR_2)\}_6]]$ / M	10^4 $[[(R_2NC(S)S)_2]]$ / M	k_{obsd} / s^{-1}
Et	10.6	5.02	100	0.108
			200	0.187
			300	0.221
			400	0.262
			500	0.270
	15.2	5.02	100	0.179
			200	0.271
			300	0.357
			400	0.421
			500	0.468
	20.3	5.02	100	0.302
			200	0.456
			300	0.562
			400	0.669
			500	0.724
	25.0	5.02	200	0.788
			300	0.980
			400	1.13
			500	1.30
n-Pr	10.3	5.00	100	0.0993
			200	0.136
			299	0.164
			400	0.205
			500	0.235
	15.2	5.00	100	0.163
			200	0.261
			299	0.315
			400	0.321
			500	0.360
	20.0	5.00	100	0.289
			200	0.414
			299	0.482
			400	0.585
			500	0.670
n-Pr	25.1	5.00	100	0.503
		10.0		0.501
		5.00	200	0.673
		10.0		0.786
		5.00	300	0.942
		10.0		0.828
	25.1	5.00	400	1.04
		10.0		0.952
		5.00	500	1.04
		10.0		1.11
i-Pr	10.2	4.99	100	0.762
			201	1.01
			301	1.17
			400	1.32
			501	1.40
	14.9	4.99	100	1.15
			201	1.55
			301	1.84
			400	2.01
			501	2.22
	20.0	5.00	100	1.91
			201	2.55
			301	2.92
			400	3.13
			501	3.36
	25.1	5.00	100	3.03
			201	4.12
			301	4.68
			400	5.05
			501	5.54

absorption maximum at *ca.* 600 nm, which has been assigned to the $[Ag(S_2CNR_2)_2]$ complex.[15,18] Thus, stoichiometry for the reaction of $[\{Ag(S_2CNR_2)\}_6]$ with $[(R_2NC(S)S\rbrace_2]$ (R=Et, *n*-Pr, and *i*-Pr) is expressed as Eq. 7. The equilibrium constants K in

$$\frac{1}{6}[\{Ag(S_2CNR_2)\}_6] + \frac{1}{2}[(R_2NC(S)S\rbrace_2] \overset{K}{\rightleftarrows} [Ag(S_2CNR_2)_2] \quad (7)$$

chloroform at 20 °C (see Table 3) were determined spectrophotometrically by Åkerström.[15] We determined the K value in dichloromethane at four different temperatures by the same method (Table 3). Plots of $\ln K$ *vs.* $1/T$ for each system gave a linear relation, from which thermodynamic parameters of the reaction 7 were obtained. The results are given in Table 3, which indicates that the equilibrium lies so far to the left. The fact that the K value for R=*i*-Pr is larger than those for R=*n*-Pr and Et may be due to a larger inductive effect of the isopropyl group than the propyl and ethyl groups of the dithiocarbamate ligands, resulting in increasing stability of $[Ag(S_2CNR_2)_2]$ by delocalization of electronic charges from the dithiocarbamate ligand to Ag(II).

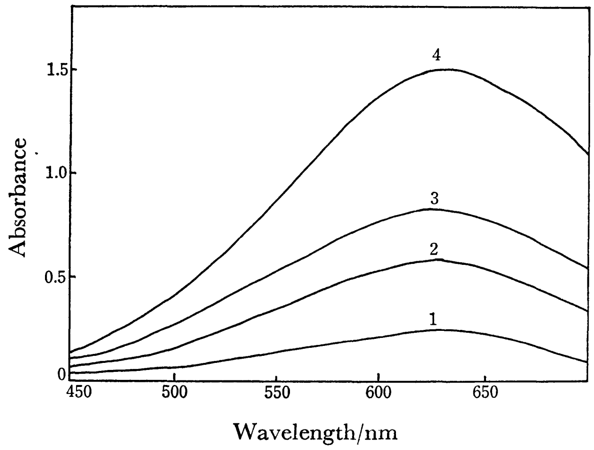

Fig. 3. Rapid scanning spectra after mixing $[\{Ag(S_2CN\text{-}i\text{-}Pr_2)\}_6]$ (5.0×10^{-4} M) with $[(i\text{-}Pr_2NC(S)S\rbrace_2]$ (5.0×10^{-2} M) in CH_2Cl_2 at 25 °C; cell length=2 mm. 1: 0.1 s, 2: 0.2 s, 3: 0.3 s, 4: 1.0 s.

A typical change of electronic spectra in the visible region after mixing of the reactants is depicted in Fig. 3, which clearly shows the formation of $[Ag(S_2CN\text{-}i\text{-}Pr_2)_2]$ (λ_{max}=620 nm, $\varepsilon_{max}=1.3\times10^4$ M^{-1} cm^{-1} in CH_2Cl_2; lit,[15] λ_{max}=620 nm in $CHCl_3$). The rate of reaction was, therefore, followed by measuring the absorbance at 620 nm (R=*i*-Pr) or 600 nm (R=Et and *n*-Pr). Plots of $\ln(A_\infty - A_t)$ *vs.* time were found to be linear to at least 80% completion except for the initial short period after mixing, as in the case of copper complexes (Fig. 2). Pseudo-first-order rate constants obtained from a linear region of the plots are listed in Table 4. Plots of k_{obsd} *vs.* the concentration of $[(R_2NC(S)S\rbrace_2]$ showed pronounced curvature at high concentrations of $[(R_2NC(S)S\rbrace_2]$. A typical example is shown in Fig. 4, which is in contrast with the linear relationship for the copper system. This notable difference can be explained by the assumption that the multi-step equilibrium constant K_0 appearing in Eq. 5 is larger in the silver system than in the copper system.

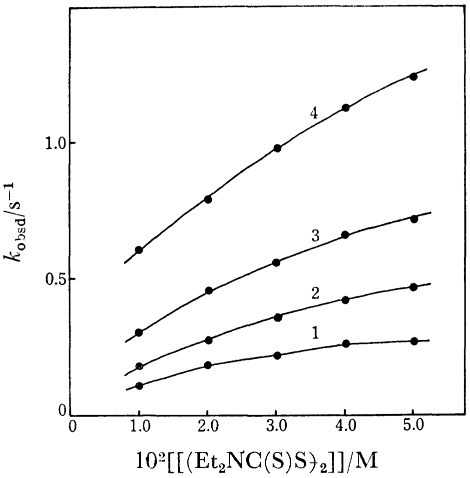

Fig. 4. Plots of k_{obsd} *vs.* $[[(Et_2NC(S)S\rbrace_2]]$ for the reaction of $[\{Ag(S_2CNEt_2)\}_6]$ with $[(Et_2NC(S)S\rbrace_2]$ in CH_2Cl_2; $[[\{Ag(S_2CNEt_2)\}_6]]=5.0\times10^{-4}$ M. 1: 10.6 °C, 2: 15.2 °C, 3: 20.3 °C, 4: 25.0 °C.

The mechanism proposed above for the copper complexes is, therefore, applicable to the silver complexes; the reaction pathways can be postulated as Eqs. 8 and 9, followed by dimerization of the $[R_2NCS_2\cdot]$

$$[\{Ag(S_2CNR_2)\}_6] \overset{+[(R_2NC(S)S\rbrace_2]}{\rightleftarrows} [Ag(S_2CNR_2)\{(R_2NC(S)S\rbrace_2\}] + [\{Ag(S_2CNR_2)\}_5] \overset{+[(R_2NC(S)S\rbrace_2]}{\rightleftarrows} \cdots\cdots \; K_0, \quad (8)$$

$$[Ag(S_2CNR_2)\{(R_2NC(S)S\rbrace_2\}] \xrightarrow{k} [Ag(S_2CNR_2)_2] + [R_2NCS_2\cdot] \quad (9)$$

radical (Eq. 4). Moreover, the bivalent silver complex, $[Ag(S_2CNR_2)_2]$, formed by Eq. 9 is expected to degrade because of its instability around room temperature. Similar instability has been reported for bis(diethylthiocarbamato)copper(II),[23] which rapidly rearranges into a hexameric univalent copper complex according to Eq. 10. By analogy with this, $[Ag(S_2CNR_2)_2]$ is suggested to rearrange as shown in Eq. 11. Equation 11 displays a unimolecular rearrangement of the

$$[Cu(SOCNEt_2)_2] \longrightarrow \frac{1}{6}[\{Cu(SOCNEt_2)\}_6] + \frac{1}{2}[(Et_2NC(O)S\rbrace_2] \quad (10)$$

$$[Ag(S_2CNR_2)_2] \xrightarrow{k'} \frac{1}{6}[\{Ag(S_2CNR_2)\}_6] + \frac{1}{2}[(R_2NC(S)S\rbrace_2] \quad (11)$$

Ag(II) complex into the hexameric Ag(I) complex and tetraalkylthiuram disulfide with the rate constant of k', though the mechanism has not been clarified in the present work. The Ag(II) complex is possible also to react with the dialkyldithiocarbamato radical produced by Eq. 9, bimolecularily with the rate constant of k'', affording the Ag(I) hexamer, as shown in Eq. 12. It is not obvious, however, which of Eqs. 11

$$[Ag(S_2CNR_2)_2] + [R_2NCS_2\cdot] \xrightarrow{k''} \frac{1}{6}[\{Ag(S_2CNR_2)\}_6] + [(R_2NC(S)S\}_2] \quad (12)$$

and 12 is predominant in the silver system. If one assumes $k \gg k'$ and/or k'', then k_{obsd} in the presence of excess $[(R_2NC(S)S\}_2]$ also is given by Eq. 5. It is apparent from Eq. 5 that the plots of k_{obsd} *vs.* the concentration of $[(R_2NC(S)S\}_2]$ show a curvature at so high concentrations of $[(R_2NC(S)S\}_2]$ as $K_0[[(R_2NC(S)S\}_2]]$ can not be neglected against unity. This is consistent with the observed kinetics (Fig. 4). Equation 5 can be transformed to Eq. 13, which predicts that there should be a

$$\frac{1}{k_{obsd}} = \frac{1}{K_0k[[(R_2NC(S)S\}_2]]} + \frac{1}{k}, \quad (13)$$

linear relationship between $1/k_{obsd}$ *vs.* $1/[[(R_2NC(S)S\}_2]]$, with the intercept of $1/k$ and the slope of $1/K_0k$. As an example of the plots is depicted in Fig. 5, which shows a linear relation over the observed range of $[(R_2NC(S)S\}_2]$ concentrations. The rate and equilibrium constants for the $[\{Ag(S_2CNR_2)\}_6]$-$[(R_2NC(S)S\}_2]$ system are summarized in Table 5.

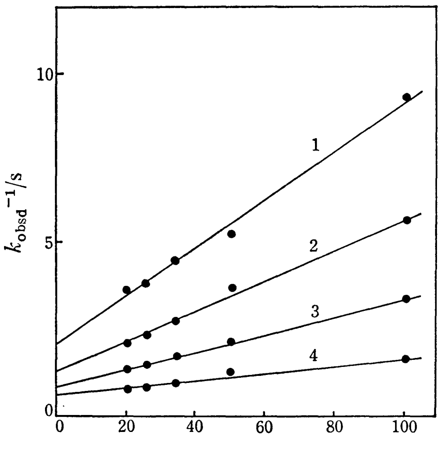

Fig. 5. Plots of $1/k_{obsd}$ *vs.* $1/[[(Et_2NC(S)S\}_2]]$ for the reaction of $[\{Ag(S_2CNEt_2)\}_6]$ with $[(Et_2NC(S)S\}_2]$ in CH_2Cl_2; $[[\{Ag(S_2CNEt_2)\}_6]] = 5.0\times10^{-4}$ M. 1: 10.6 °C, 2: 15.2 °C, 3: 20.3 °C, 4: 25.0 °C.

Table 5. Equilibrium and rate constants for the reaction of $[\{Ag(S_2CNR_2)\}_6]$ with $[(R_2NC(S)S\}_2]$ in CH_2Cl_2[a)]

R	Temp °C	K_0 M^{-1}	k s^{-1}
Et	25.0	28.2± 4.2	2.17±0.30
	20.3	38.4± 3.9	1.08±0.10
	15.2	31.8± 5.0	0.74±0.11
	10.6	30.4± 4.7	0.47±0.07
n-Pr	25.1	49.1±12.3	1.50±0.34
	20.0	48.8± 9.0	0.87±0.15
	15.2	45.6± 6.5	0.53±0.68
	10.3	47.9±11.6	0.30±0.07
i-Pr	25.1	86.7± 5.3	6.57±0.31
	20.0	89.4± 4.6	4.03±0.16
	14.9	71.2± 6.5	2.73±0.21
	10.2	79.6± 8.3	1.70±0.13

a) Errors quoted are standard deviations.

Thermodynamic and activation parameters calculated from K_0 and k at four different temperatures (Table 5) are listed in Table 6, which reveals that the $\Delta H°_{(K_0)}$ values are near to zero. The $\Delta S°_{(K_0)}$ term is, therefore, a dominant factor to cause the reaction 8. The positive $\Delta S°_{(K_0)}$ values are consistent with the stepwise dissociation of $[\{Ag(S_2CNR_2)\}_6]$ by the attack of $[(R_2NC(S)S\}_2]$. The small negative $\Delta S^{\ddagger}_{(k)}$ values suggest that the configuration of the adduct formed between monomeric $[Ag(S_2CNR_2)]$ and thiuram disulfide, as shown in **3** or **4**, is essentially maintained in the transition state of reaction 9.

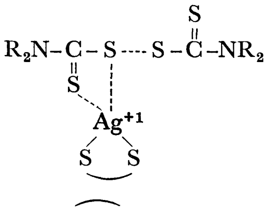

3: $\widehat{S\quad S} = S_2CNR_2$

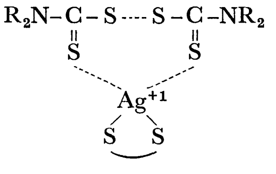

4

Finally, it should be mentioned that the K_0k values for the copper system are about two orders greater than those for the silver system under similar experimental conditions (Tables 2 and 5). In addition, a linear dependence of k_{obsd} on the concentration of thiuram disulfide observed for the copper system predicts that the K_0 value is not so large as that for the silver system, as described above. Thus, the k values for the copper system must be more than two orders greater than those for the silver system. This is in agreement with the fact that the oxidation to a bivalent state is easier in Cu(I) complexes than in Ag(I) complexes.[24)]

Table 6. Thermodynamic and activation parameters for the reaction of $[\{Ag(S_2CNR_2)\}_6]$ with $[(R_2NC(S)S\}_2]$ in CH_2Cl_2 at 25 °C[a)]

R	$\Delta H°_{(K_0)}$ kJ mol^{-1}	$\Delta S°_{(K_0)}$ J mol^{-1}K^{-1}	$\Delta H^{\ddagger}_{(k)}$ kJ mol^{-1}	$\Delta S^{\ddagger}_{(k)}$ J mol^{-1}K^{-1}
Et	−1±7	29±50	70±4	−4±28
n-Pr	2±1	38±10	74±1	−2± 5
i-Pr	6±4	59±29	59±1	−32± 8

a) Errors quoted are standard deviations.

The authors are grateful to the Ministry of Education for support of this work through Grant-in-Aid for Scientific Research.

References

1) B. L. Edgar, D. J. Duffy, M. C. Palazzotto, and L. H. Pignolet, *J. Am. Chem. Soc.*, **95**, 1125 (1973).

2) A. Avdeef, J. P. Fackler, Jr., and R. G. Fischer, Jr., *J. Am. Chem. Soc.*, **92**, 6972 (1970).

3) D. Coucouvanis, *Prog. Inorg. Chem.*, **11**, 233 (1970).

4) J. Willemse, J. A. Cras, J. J. Steggerda, and C. P. Keijzers, *Structure and Bonding*, **28**, 83 (1976).

5) E. A. Pasek and D. K. Straub, *Inorg. Chim. Acta*, **21**, 23 (1977).

6) B. M. Mattson and L. H. Pignolet, *Inorg. Chem.*, **16**, 488 (1977).

7) E. W. Ainscough and A. M. Brodie, *J. Chem. Soc., Dalton Trans.*, **1977**, 565.

8) S. H. Wheeler, B. M. Mattson, G. L. Miessler, and L. H. Pignolet, *Inorg. Chem.*, **17**, 340 (1978).

9) G. A. Katsoulos, G. E. Manoussakis, and C. A. Tsipis, *Inorg. Chim. Acta*, **30**, L295 (1978).

10) H. Kita, K. Tanaka, and T. Tanaka, *Bull. Chem. Soc. Jpn.*, **48**, 2816 (1975).

11) H. Kita, K. Tanaka, and T. Tanaka, *Inorg. Chim. Acta*, **21**, 229 (1977).

12) H. Kita, K. Itoh, K. Tanaka, and T. Tanaka, *Bull. Chem. Soc. Jpn.*, **51**, 3530 (1978).

13) A. R. Hendrickson, R. L. Martin, and N. M. Rohde, *Inorg. Chem.*, **15**, 2115 (1976).

14) S. Åkerström, *Arkiv Kemi*, **14**, 387 (1959).

15) S. Åkerström, *Arkiv Kemi*, **14**, 403 (1959).

16) R. Pettersson and T. Vänngård, *Arkiv Kemi*, **17**, 249 (1961).

17) T. R. Reddy and R. Srinivasan, *J. Chem. Phys.*, **43**, 1404 (1965).

18) M. V. Rajasekharan, C. N. Sethulakshmi, P. T. Manoharan, and H. Gudel, *Inorg. Chem.*, **15**, 2657 (1976).

19) H. C. Brinkhoff, J. A. Cras, J. J. Steggerda, and J. Willemse, *Recl. Trav. Chim. Pays-Bas*, **88**, 633 (1969); H. C. Brinkhoff, J. A. Cras, J. J. Steggerda, and J. Willemse, *ibid.*, **89**, 11 (1970); P. T. Beurskens, J. A. Cras, J. H. Noordik, and A. M. Spruijt, *J. Cryst. Mol. Struct.*, **1**, 93 (1971); C. Chieh, *Can. J. Chem.*, **55**, 1115 (1977).

20) H. Coutreras and H. Cortés, *Inorg. Nucl. Chem. Lett.*, **6**, 225 (1970).

21) R. M. Golding and W. C. Tennant, *Mol. Phys.*, **24**, 301 (1972); R. A. Palmer, W. C. Tennant, M. F. Dix, and A. D. Rae, *J. Chem. Soc., Dalton Trans.*, **1976**, 2345.

22) G. Cauquis and D. Lachenal, *J. Electroanal. Chem. Interfacial Electrochem.*, **43**, 205 (1973).

23) S. Åkerström, *Arkiv Kemi*, **24**, 479 (1965).

24) F. A. Cotton and G. Wilkinson, "Advanced Inorganic Chemistry," 3rd ed, Interscience, New York (1972), pp. 905 and 1044.